0181

FRACTURE AND PLASTIC DEFORMATION CAPACITY OF THE WELDED JOINT OF COMPOSITE BEAM-TO-STEEL COLUMN CONNECTIONS

Akira MATSUO[1], Yuji NAKAMURA[2], Takao TAKAMATSU[3] And Yoshimasa MATSUI[4]

SUMMARY

Many brittle fractures at the bottom flange of steel beams were found in Northridge and Hyogoken-Nanbu Earthquakes. Though it has been discussed that the effect of concrete slab resulted in the fractures of the bottom flange, there are only a few reports on the fracture of the composite beam-to-steel column subassemblages. On the other hand it was also discussed that an early yielding of the connection panel give rise to local deformation at the beam-to-column welded joint, which might be one of the causes for joint fractures. In this research four T-shaped composite beam subassemblages of strong panel, are tested. The column of these specimens is made of H-section(H-series) or built-RHS(S-series) or cold roll formed RHS(R-series). Additional two steel beam specimens for each series and five specimens of weak panel type for H- and S-series are also tested. These beams are made of SN400B or SN490B, which has high notch toughness. All bottom flanges of the composite beam sustained local buckling in negative bending and were broken in the following positive bending cycles, which is also an observed phenomenon in Hyogoken-Nambu Earthquake. According to comparison of the steel and composite beam subassemblages of a strong panel type, accumulated plastic deformation capacities ƒÅ and ƒÅs of the composite beam obtained from cyclic and skeleton curve, respectively, range 30 to 70% of that of steel beam, some of which don't satisfy the required value in the aseismic design in Japan. According to the specimens of weak panel type total energy dissipated by yielding of the beam and panel increased, as the shear strength of the panel decreased.

INTRODUCTION

Aseismic resistance of a steel building is secured by assurance of enough strength and deformation capacity of component members and connections. Many brittle fractures following to some plastic deformation were found at the bottom flange of steel beams in Hyogoken-Nanbu Earthquake[AIJ,1995]. Many full-scale experimental tests were performed to know the deformation capacity of steel beams[AIJ,1997]. On the other hand there were only a few tests[Kaneko, 1998] on composite beam subassemnblages, where the deformation capacity of the beam might be greatly reduced. It was also discussed that an early yielding of the connection panel give rise to local deformation at the beam-to-column welded joint, which might be one of the causes for joint fractures.

In this research nine T-shaped composite beam subassemblages are tested consisting of three groups H series(built-H column-H beam), S series (built-RHS column-H beam) and R series(cold roll formed RHS column-H beam). The panel strength ranges from 0.6 to 1.8 times as large as beam strength. Additional two steel beam specimens of strong panel for each series are also tested.

[1] *Department of Structural Engineering, Hiroshima University, Higashi-Hiroshima, Japan Email:matu12@ipc.hiroshima-u.ac.jp*
[2] *Department of Structural Engineering, Hiroshima University, Higashi-Hiroshima, Japan*
[3] *Department of Civil Engineering, Hiroshima Institute of Technology, Hiroshima, Japan*
[4] *Keisoku Research Consultant Co., Hiroshima, Japan*

EXPERIMENTAL PLAN

Standard shape of the specimen is illustrated in Figure 1. Combination of the beam and column and further details of the specimens are listed in Table 1, in which the panel yield ratio R_{py} is calculated according to equation (1). P_{py} and P_{by} are the loads when the panel and beam reach to the yield moment ${}_pM_y$ and ${}_bM_y$, where ${}_pM_y$ is given by eq.(2). The effective volume V_p of the panel plate in calculating yield panel moment of the composite beam specimen is obtained as the volume of the panel plate extended to the center of the concrete slab. Each R_{py} of H and S series is achieved by changing the material and thickness of the column web, while the flange thickness is kept the same. Each column section is chosen to be in elastic range during whole period of the experimental test. The first letter of the specimen's name indicates column (H: built-H, S: built-RHS, R: cold roll formed RHS), and the following two numbers indicate R_{py}. The name with N in the next position indicates a steel beam specimen. The number in the last position identifies the two same specimens. The numbers of stud connectors are determined to be able to resist more than maximum compressive strength of the concrete slab at the face of the column flange.

$$R_{py} = P_{py} / P_{by} \quad (1), \qquad {}_pM_y = V_p f_y / \sqrt{3} \quad (2)$$

The details of welded joint of three series are illustrated in Fig.2. The joint of H-series is welded flange-bolted web (WF-BW) type, that of S-series is welded flange-welded web (WF-WW) type, and that of R series is WF-WW type with through diaphragms. The shape of scallop is a conventional type following to JASS6 in Japan. CO_2 gas shielded arc welding is applied to the full-penetration weld, where an electric current is kept about 40V and 300A, inter-pass temperature is less than $350°C$, and heat input introduced by welding is kept 10 to 17 kJ/cm. Layers of passes of full-penetration weld in the beam flange is also illustrated in Fig.2.

Mechanical properties of each material are shown in Tab.2. Tab. 3 shows chemical composition of the beam(SN400B or SN490B) according to the mill sheet. Fig. 3 shows three positions, base metal, fillet part and HAZ of the beam flange, from which Charpy test specimens, JIS No.4 test specimens, are extracted. Three

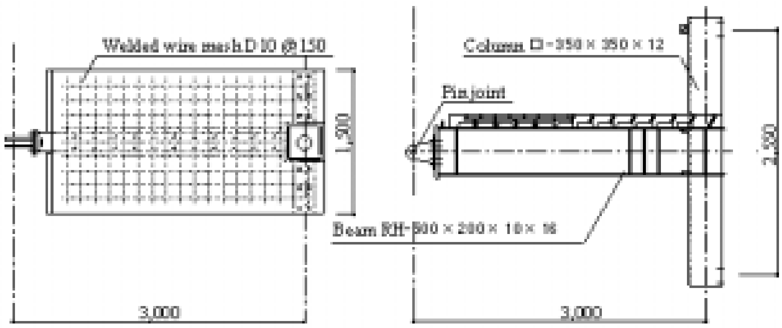

Figure 1 Shape and size of specimens

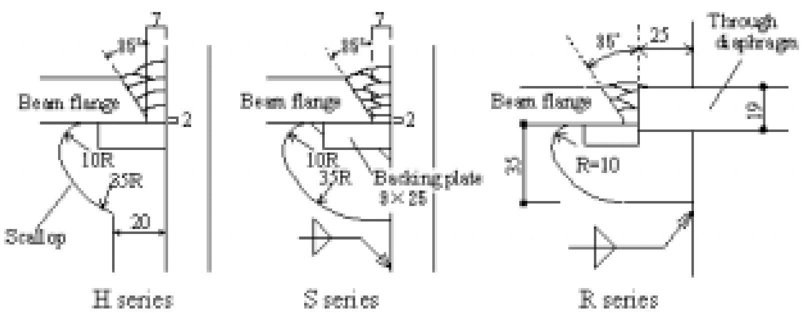

Figure 2 Details of beam-to-column joint

specimens are tested for each temperature and the transition curve is determined by the least square method Fig.4 and Tab.4 show that the beam flange has high notch toughness.

Top and bottom of the column are simply supported to the loading frame, and the top of the beam is loaded cyclically through the oil jack. Loading program is illustrated in Fig.5, where δ and δ_p are the total displacement of the frame and elastic displacement of the steel frame corresponding to the plastic moment M_p at the critical section of the beam.

Table 1 Details of Specimens

Specimen	Joint	R_{py} (steel)	R_{py} (slab)	Beam	Column	Panel	Slab
H07	WF-BW	0.72	0.81	$H-500\times200\times10\times16$ $(SN490B)$	$H-350\times350\times12\times16$	SM490A	90
H09		0.91	1.02		$H-350\times350\times16\times16$	SM490A	90
H18		1.78	1.99		$H-350\times350\times16\times16$	2-DP9	90
H18-N1		1.78	-		$H-350\times350\times16\times16$	2-DP9	0
H18-N2		1.78	-		$H-350\times350\times16\times16$	2-DP9	0
S06	WF-WW	0.60	0.67	$H-500\times200\times10\times16$ $(SN490B)$	$RHS-350\times350\times6\times16$	SS400	90
S08		0.75	0.83		$RHS-350\times350\times6\times16$	SM490A	90
S10		0.93	1.03		$RHS-350\times350\times9\times16$	SS400	90
S15		1.52	1.70		$RHS-350\times350\times12\times16$	SM490A	90
S15-N1		1.52	-		$RHS-350\times350\times12\times16$	SM490A	0
S15-N2		1.52	-		$RHS-350\times350\times12\times16$	SM490A	0
R16-1	WF-WW	1.56	1.69	$H-500\times200\times10\times16$ $(SN400B)$	$RHS-350\times350\times12\times12$	BCR295	90
R16-2		1.56	1.69		$RHS-350\times350\times12\times12$	BCR295	90
R16-N1		1.56	-		$RHS-350\times350\times12\times12$	BCR295	0
R16-N2		1.56	-		$RHS-350\times350\times12\times12$	BCR295	0

Table 2 Mechanical properties of materials

(unit : tf/cm^2, kgf/cm^2)

Column(H series)	σ_y	σ_u	Column(S series)	σ_y	σ_u
9mm(SM490A)	4.12	5.47	6mm(SS400)	2.99	4.43
12mm(SM490A)	3.63	5.45	9mm(SS400)	3.10	4.73
16mm(SM490A)	3.43	5.21	6mm(SM490A)	3.76	5.35
Beam(SN490B)	3.65	5.32	12mm(SM490A)	3.82	5.25
Beam(SN400B)	3.22	4.60	16mm(SM490A)	3.37	5.27
Concrete(H series)	Fc=396		Column(R series)	3.83	4.62
Concrete(S series)	Fc=291		Concrete(R series)	Fc=346	

Table 3 Chemical compositions of steel beam

Mill Sheet	C	Si	Mn	P	S	Cu	Ni	Cr	V	Nb	Mo	Ceq
	$\times100$			$\times1000$		$\times100$			$\times1000$			$\times100$
SN490B	16	39	141	20	7	1	2	4	43	1	1	42
SN400B	15	20	73	23	7	2	2	4	3	1	11	29

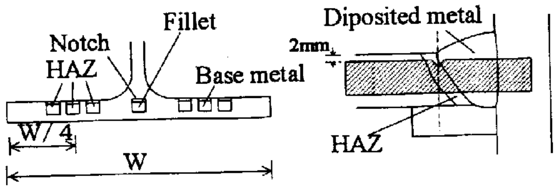

Figure 3 Positions where Charpy specimens are extracted

Table 4 Fracture toughness of steel

Material		Fillet	Base metal	HAZ	Mill sheet
SN490B	$_vE_0(J)$	173	238	162	230
	$_vT_E(°C)$	-11.0	-14.4	-9.4	-
SN400B	$_vE_0(J)$	148	241	-	203
	$_vT_E(°C)$	-2.5	10.6	-	-

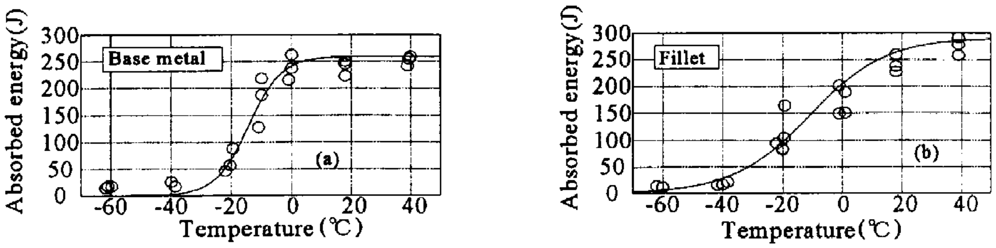

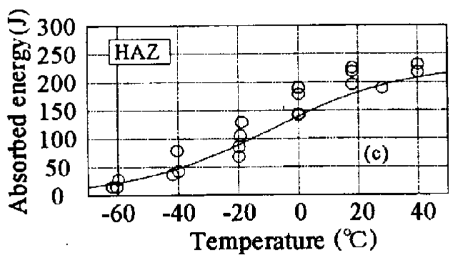

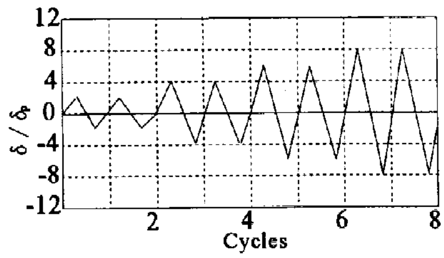

Figure 4 Energy transition curve(SN490B)

Figure 5 Loading program

3. EXPERIMENTAL RESULTS AND DISCUSSIONS

3.1 EXPERIMENTAL RESULTS

Representative load P - total displacement δ curves and beam moment M - rotation θ curves are illustrated i Fig.6. Beam deformation decreases, as the panel strength decreases. Experimental results are summarized in

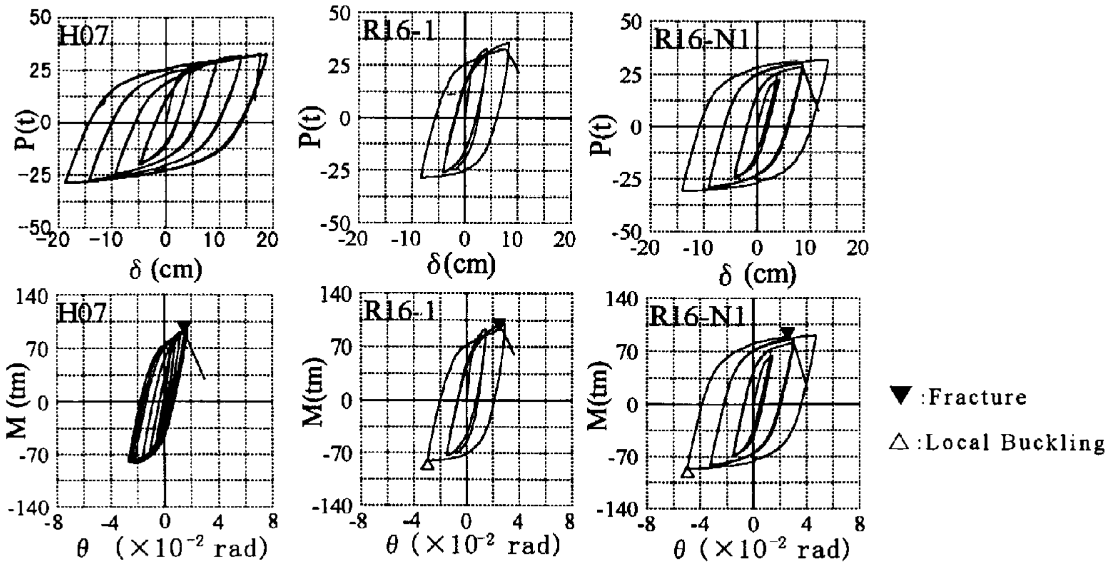

Figure 6 Deformation of the frame and beam

Tabs.5 and 6. In these tables $_cP_{by}$, $_cP_{bp}$ and $_cP_{py}$ are the loads corresponding to calculated yield and plastic strengths of the beam and calculated plastic strength of the panel. $_cP_{bp}$ of the RHS column specimens are. calculated according to [Tateyama,1988]. Experimental yield loads $_eP_{by}$ are obtained as the points whos tangent modulus is reduced to 1/3 or 1/5 of elastic modulus. In Tab.6 $8\delta_p+5$ indicates the 5th positive loadin cycle of $8\delta_p$ amplitude. The fracture line initiated from the scallop or weld toe of the exterior part of the beai flange and passed through the HAZ or base metal of the beam flange. Fracture of the composite beam of th strong panel frames occurred to bottom flange in positive bending after local buckling in preceding negativ bending cycles, which was also an observed phenomenon in Hyogoken-Nambu Earthquake

Table 5 Experimental results (1)

(Unit: tonf)

Specimens	$_cP_{by}$	$_cP_{bp}$	$_cP_{py}$	$_eP_y(1/3)$	$_eP_y(1/5)$	$_eP_{max}$
H07	28.5	44.5	23.1	22.9	24.5	33.0
H09			29.1	28.0	29.5	36.6
H18			56.8	32.5	36.9	44.8
H18-N1	24.9	28.2	44.3	26.5	28.5	35.1
H18-N2				26.0	28.4	36.3
S06	28.5	39.2	19.1	18.7	19.9	30.8
S08			23.9	21.7	23.4	34.1
S10			29.6	26.6	28.0	39.7
S15			48.6	28.8	31.9	42.2
S15-N1	24.9	28.2	38.0	26.9	29.3	36.2
S15-N2				24.9	28.4	35.2
R16-1	26.0	34.5	43.9	24.7	27.2	35.6
R16-2				24.4	28.9	37.1
R16-N1	22.0	25.2	34.2	19.4	21.0	32.0
R16-N2				20.1	21.7	32.8

Table 6 Experimental results (2)

Specimen	Temp. (°C)	Local buckling	Ultimate State
H07	11	-	$8\delta_p$ +5, LF, Brittle fracture from weld defect
H09	14	$6\delta_p$ -2	$8\delta_p$ +2, LF, Ductile fracture from scallop
H18	13	$6\delta_p$ -1	$6\delta_p$ +2, LF, Ductile fracture from scallop
H18-N1	12	$6\delta_p$ +1	$6\delta_p$ -3, Local buckling of UF and LF
H18-N2	11	$6\delta_p$ +1	$8\delta_p$ +1, LF, Ductile fracture from toe of weld
S06	9	-	$8\delta_p$ -10, Fracture of panel
S08	10	-	$8\delta_p$ -10, Fracture of panel
S10	9	$8\delta_p$ -2	$8\delta_p$ +3, LF, Ductile fracture from toe of weld
S15	8	$6\delta_p$ -1	$6\delta_p$ +2, LF, Ductile fracture from toe of weld
S15-N1	14	-	$6\delta_p$ -2, UF, Ductile fracture from weld defect
S15-N2	11	$6\delta_p$ -1	$8\delta_p$ +1, Local buckling of UF and LF
R16-1	14	$4\delta_p$ -1	$4\delta_p$ +2, LF, Ductile fracture from scallop
R16-2	13	$4\delta_p$ -1	$4\delta_p$ +1, LF, Ductile fracture from scallop
R16-N1	13	$6\delta_p$ -1	$6\delta_p$ +2, LF, Ductile fracture from scallop
R16-N2	14	$6\delta_p$ -1	$6\delta_p$ -1, UF, Ductile fracture from scallop

UF, LF show upper and lower flange

3.2 PLASTIC DEFORMATION CAPACITY OF THE BEAM

Experimental accumulated plastic deformation capacities η , η_s^+, η_s^- and η_s of the beam in the strong pane frames are listed in Tab.7. η is given by eq.(3), where W_i^+ and W_i^- are the energy dissipated in positive an negative bending of i-th cycle of beam $M-\theta$ curve in Fig.7, respectively. η_s^+, η_s^- and η_s are given by eqs.(4 and (5), where W_s^+ is the shaded area under the skeleton curve in Fig.7. Those η , η_s^+ and η_s of composit beams are reduced to maximum 50, 30 and 40% of steel beams, respectively. The accumulated plasti deformation capacity η_R required to the strong-column weak-beam frames expected high deformability(Rank I is given by eq.(7) and is 5.0 according to aseismic design[AIJ,1990] in Japan. As η includes energy dissipatio in the Bauschinger area, η is interpreted to be equivalent to $a_b\eta_s$. According to Tab.7 and eq.(7), η_s of R16 1,2 don't satisfy η_R =5.0 required to the frames in Rank I, but η is barely enough to secure it. Fig.8 shows th effects of the panel shear deformation on the energy absorbing capacity of the total frame until the fracture c the connection, where η_{b+p} is given by eq.(6). ${}_{b+p}W_i^+$ and ${}_{b+p}W_i^-$ are the energy dissipated by both the bear and panel in positive and negative loading, respectively. This suggests that the accumulated plastic deformatio capacity η_{b+p} of the total frame increases, as the panel strength decreases.

$$\eta = \sum_i (W_i^+ + W_i^-)/2M_p\theta_p \quad (3) \qquad \eta_s^{+-} = \sum W_s^{+-}/M_p\theta_p \quad (4)$$

$$\eta_s = (\eta_s^+ + \eta_s^-)/2 \quad (5), \qquad \eta_{b+p} = \sum_i ({}_{b+p}W_i^+ + {}_{b+p}W_i^-)/2M_p\theta_p \quad (6)$$

$$\eta_R = \frac{\delta_{by}}{\delta_{Ry}} a_p a_b \eta_s + a_d \quad (7)$$

δ_{by}, δ_{Ry} : yield deformation of the beam and frame($\delta_{by}/\delta_{Ry} = 1/3$)

a_p : variable to include the energy dissipation by the connection panel(=1.5)

a_b : variable to include the energy dissipation in Bauschinger area of $M-\theta$ curve(=2.0)

a_d : variable to include the energy dissipation in the degrading area(=0.0 in case of joint fracture)

η_s : accumulated plastic deformation capacity obtained from eqs.(4) and (5) of the beam

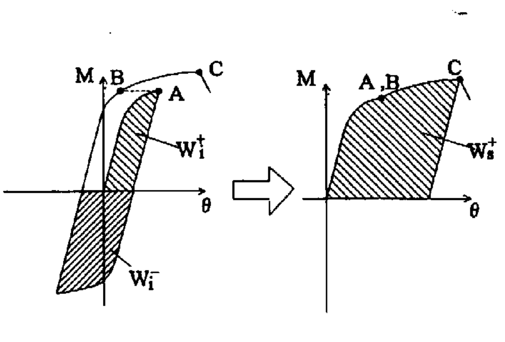

Figure 7 Cyclic and skeleton M - θ curve

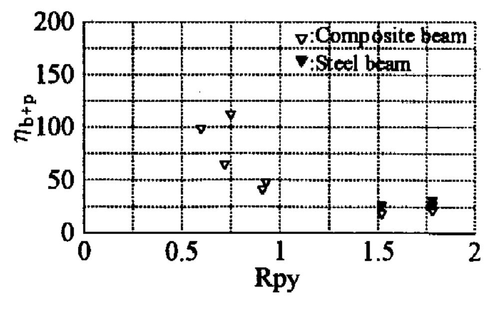

Figure 8 Accumulated plastic deformation capacity of total frames

Table 7 Accumulated plastic deformation capacity

Specimens	η	η_s^+	η_s^-	η_s
H18	21.5	6.1	5.3	5.7
H18-N1	31.5	8.3	4.9	6.6
H18-N2	27.0	7.2	8.2	7.7
S15	19.0	5.9	7.1	6.5
S15-N1	20.0	6.6	5.5	6.1
S15-N2	27.0	7.1	10.2	8.7
R16-1	11.4	3.3	5.8	4.6
R16-2	14.8	3.5	5.3	4.4
R16-N1	26.0	9.9	9.5	9.7
R16-N2	29.0	10.9	11.1	11.0

3.3 STRAIN IN THE BOTTOM FLANGE OF THE BEAM

Fig.10 shows load P - average strain ε curves in the bottom flange of R16-1 and R16-N2. Wire strain gages ai pasted at the position shown in Fig.9 from 65mm away from the column face. Applying the non-stationai stress-strain rules[Nakamura 1981] to these strain paths, stress-strain loops experienced in the bottom flange ai obtained. As it is reported that the fracture toughness of steel is reduced depending upon the experience skeleton strain[JWES APD Committee,1997], skeleton curves of stress-strain relation are formed applying th method of Fig.7 to these loops, and are illustrated in Fig.11. The marks show the cutting and connecting poin of the curve, and the numbers, for example, 4+1 mean the end of the first positive bending cycle ($4\delta_p$ amplitude. As peak strength of the second loop of the same amplitude in cyclic $M-\theta$ curve of th composite beam is smaller than the first loop in Fig.6, the second loop is completely excluded from skeleto curve. This is because the resisting mechanism of the composite beam changes at the moment of conta between column face and concrete slab, and the time of contact is slightly delayed in the second cycle. On th other hand, the second loop of the same amplitude in cyclic stress-strain curve contributes to the skeleton stres strain curve. This means η_s^+ of the composite beam gives smaller deformation capacity than the practical case.

The ratio of incremental skeleton strains in the bottom flange for each cycle between the composite beam an steel beam is listed in Tab.8, ranging from 1.6 to 2.3. While the plastic neutral axis of the composite bea calculated according to [Tateyama,1988] is in the top flange, that of steel beam is in the center of the web. If it i assumed that the amplitude of curvature within the plastic hinge doesn't change between the steel beam an composite beam, this ratio will be 2.0, which roughly corresponds to Tab.8.

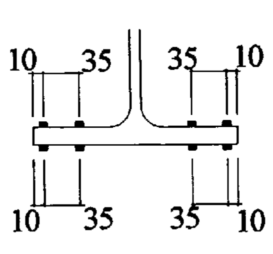

Figure 9 Strain gages in the bottom flange

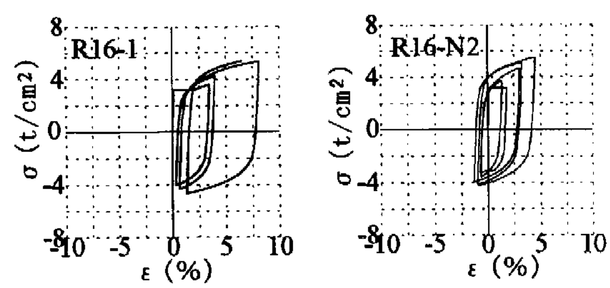

Figure 10 P - ε relation in the bottom flange

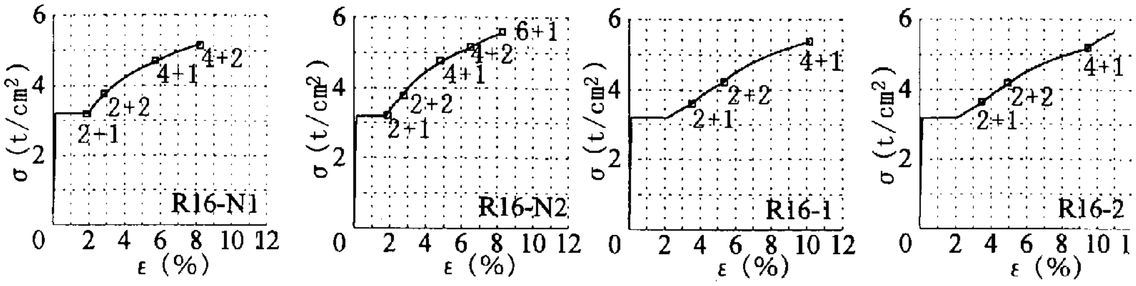

Figure 11 skeleton σ - ε relation

Table 8 Ratio of strain increment between steel and composite beam

	$2\theta_p$+1	$2\theta_p$+2	$4\theta_p$+1
R16-1/R16-N2	1.8	2.0	1.7
R16-1/R16-N2	1.9	2.0	2.3
R16-2/R16-N1	1.7	1.6	1.6
R16-2/R16-N2	1.9	1.6	2.2

4. CONCLUSIONS

Full-scale tests of composite beam subassemblages are performed and the following conclusions are derived.

1) The accumulated plastic deformation capacities η, η_s^+ and η_s of composite beam in strong panel frames aı reduced to maximum 50, 30 and 40% of steel beams, respectively

2) The accumulated plastic deformation capacity η_{b+p} equivalent to the total energy dissipation of the fram increases, as the panel strength decreases.

3)Incremental strain of skeleton stress-strain curve in the bottom flange of the composite beam is roughl predictable from that of steel beam considering the position of plastic neutral axes.

A part of this report was conducted as one of the activities of Japanese Society of Steel Construction committee on new design methods of steel connections(Chairman: Prof. K. Takanashi of Chiba Univ.) Authoı wish to acknowledge the advises of prof. K. Morita of Chiba Univ. and financial supports of Kozai Club. The also wish to acknowledge the cooperation of Mr. T. Takenouchi(Mitsubishi Heavy Industries Co.) and Mr. K Kitazono(Graduate Student of Hiroshima Univ.).

5. REFERENCES

Architectural Institute of Japan(AIJ,1990), *Ultimate strength and deformation capacity of building in seismic design*

AIJ Steel committee of the Kinki branch(1995), *Reconnaissance report on damage to steel building structure obscrbed from the 1995 Hyogoken-Nambu earthquake*

AIJ Steel committee of the Kinki branch(1997), *Full-scale test on plastic rotation capacity of steel wide-flang beams connected with square tube steel columns*

Japan Welding Engineering Society(JWES) APD committee (1997), A textbook of a seminar on steel materiɛ and earthquake damage of steel buildings

Kaneko H. et al.(1998),"Fracture behavior of beam-to-column connections with low toughness steel' *Summaries of technical papaers of annual meeting of the AIJ*, pp409-410

Nakamura T. et al. (1981), "A non-stationary hysteretic uniaxial constitutive law and its application to numericɛ analysis of frame members Part I", *Transaction of the AIJ*, No.300, pp11-18

Tateyama E. et al.(1988), "Study on ultimate bending strength and deformation capacity of H-shaped beaı connected to RHS column with through diaphragms", *Journal of structural and construction engineering(Tran: of AIJ)*, No.389, pp109-121